Electron Localization Function From Density Components

Julien Pilmé [1]

[1] Sorbonne Universités, UPMC Univ Paris 06, CNRS, Laboratoire de Chimie Théorique
CC 137 – 4, place Jussieu F. 75252 PARIS CEDEX 05 - France
E-mail: *pilme@lct.jussieu.fr*

ABSTRACT

This work addresses the decomposition of the Electron Localization Function (ELF) into partial density contributions using an appealing split of kinetic energy densities. Regarding the degree of the electron localization, the relationship between ELF and its usual spin-polarized formula is discussed. A new polarized ELF formula, built from any subsystems of the density, and a localization function, quantifying the measure of electron localization for only a subpart of the total system are introduced. The methodology appears tailored to describe the electron localization in bonding patterns of subsystems, such as the local nucleophilic character. Beyond these striking examples, this work opens up opportunities to describe any electronic properties that depend only on subparts of the density in atoms, molecules or solids.

I. Introduction

Over the two past decades, the analysis of the gradient field of the Electron Localization Function (ELF) has helped in understanding the concept of electron-pair localization in numerous molecules and solids.[1-4] However, the long-running debate over critics of ELF about its definitions and its physical interpretations is still relevant.[5-12] These include the original formulation of Becke and Edgecombe which lies on the conditional same-spin pair probability D_σ scaled by the homogeneous electron gas (HEG) kinetic energy density $D^0{}_\sigma$[13], both D_α and D_β being separately computed. The kernel χ_σ of ELF is then expressed from n_σ occupied molecular orbitals $\varphi_{i\sigma}$, as follows:

$$\chi_\sigma = \frac{D_\sigma}{D_\sigma^0} = \frac{\sum_i^{n_\sigma} |\nabla\varphi_{i\sigma}|^2 - \frac{1}{4}\frac{|\nabla\rho_\sigma|^2}{\rho_\sigma}}{D_\sigma^0} = \frac{\tau_\sigma - \frac{1}{8}\frac{|\nabla\rho_\sigma|^2}{\rho_\sigma}}{c_f\ 2^{2/3}\ \rho_\sigma{}^{5/3}}$$

$$\text{and } ELF_\sigma = \frac{1}{1+\chi_\sigma^2} \qquad (1)$$

where ρ_σ is the σ-spin density and τ_σ is the spin contribution to the positive definite kinetic energy density. ELF_σ ranges from 0 to 1 where 1 is a situation void of Pauli repulsion, i.e. a high probability of finding electron localization. Several theoretical studies have shown that the separated $ELF_{\alpha/\beta}$ components are quite useful to evaluate the localization of unpaired electron in radicals.[14-16] In a similar manner, $ELF_{\sigma/\pi}$ components were conducted from ρ_σ/ρ_π groups of molecular orbitals. [14,15,17,18] These latter studies have been mainly motivated by the lack of assessment on the individual σ/π bonding pictures in ELF based on the total electron density (see below). They have notably proved to be meaningful to quantify the concept of resonance and to rationalize the aromaticity of ring molecules. Note that $ELF_{\sigma/\pi}$ components are in general isotopological to the termed ELI-D function which can be exactly decomposed as a sum of partial orbital contributions[19-21]. ELI-D is a variant form of the Electron Localizability Indicator (ELI), this latter being derived from the

electron pair density without any reference to the uniform electron gas.

Turning to the original definition in terms of σ-spin density, a functional form of ELF based on the total electron density can be obtained for the closed-shell systems in which $\rho_\alpha = \rho_\beta = \rho/2$. In this latter case, the kernel of this total ELF becomes:

$$\chi = \frac{\tau - \frac{1}{8}\frac{|\nabla\rho|^2}{\rho}}{c_f\rho^{5/3}} \text{ and ELF} = \frac{1}{1+\chi^2} \qquad (2)$$

where τ is the positive definite kinetic energy density and ρ is the total electron density. Note that equation (2) cannot be derived from any components of the total density, such as ρ_σ/ρ_π, and it should be strictly restricted to closed-shell systems. Actually, the equation (2) is also thoroughly used for open-shell systems because it can be obtained in a conceptually different way. Indeed, a physical interpretation of equation (2) was later attributed[22] in terms of the local kinetic energy densities as:

$$\chi = \frac{\tau^{\text{Pauli}}}{\tau^{\text{h}}} = \frac{\tau - \tau^{\text{w}}}{\tau^{\text{h}}} = \frac{\tau - \frac{1}{8}\frac{|\nabla\rho|^2}{\rho}}{c_f\rho^{5/3}} \qquad (3)$$

Where τ^w is the von Weizsäcker kinetic energy density, i.e. the kinetic energy of a density model system in which the antisymmetry is switched off.[23] The kernel χ is now interpreted in terms of Pauli kinetic energy density τ^{Pauli}, i.e. the local excess kinetic energy due to the Pauli exclusion principle. Note that some years later, ELF was also extended to *ab initio* correlated wave functions [24].

In its original definition (equation 1) as well as in its functional form (equation 3), ELF does not necessarily go to zero for vanishing density. Numerical instabilities can also appear in low density regions, typically when D_σ tends to zero faster than ρ. To address these issues, Savin et al. have introduced in the equation (3), a shifting constant $\varepsilon = 2.871.10^{-5}$ to τ^{Pauli} quantity[25]. This compels ELF to be less than 0.5 when $\rho \leq 10^{-3}$ bohr^{-3} and yields ELF to zero with the electron density.

The kinetic energy interpretation of the total ELF (equations 3) extends its validity of systems where τ^{Pauli} can be properly evaluated within Density Functional Theory, the σ dependence (equation 1) no longer appearing in the equations (2) and (3). Thus, details about bond pictures obtained from individual orbital contributions such as the σ/π decomposition, are lost in the total ELF[17]. Actually, the way to decompose the function into any density components is unclear, the total ELF being neither the sum nor the average of its partial density contributions. However, in analogy to the spin-density functional theory[26], a such decomposition in terms of spin densities (spin-polarized ELF) was proposed by Kohout and Savin[27] as follows:

$$\chi_s = \frac{\tau_\alpha^{\text{Pauli}} + \tau_\beta^{\text{Pauli}}}{\tau_\alpha^{\text{h}} + \tau_\beta^{\text{h}}} = \frac{\tau - \frac{1}{8}\frac{|\nabla\rho_\alpha|^2}{\rho_\alpha} - \frac{1}{8}\frac{|\nabla\rho_\beta|^2}{\rho_\beta}}{2^{2/3}c_f\left(\rho_\alpha^{5/3} + \rho_\beta^{5/3}\right)} \qquad (4)$$

$$\text{and ELF}_s = \frac{1}{1+\chi_s^2}$$

Note that ELF_s is also computed with the shifting constant introduced by Savin et al[25]. Although the equation (4) addresses the challenge to decompose the total ELF in terms of spin densities, the relationship between equations (3) and (4) remains unclear because it is only possible once again to obtain $\chi_s = \chi$ in the closed-shell systems. In open-shell systems, these equations generally differ.

The purpose of the present paper is to discuss the relationship between the total ELF and its partial density components. A particular focus on the relationship between the spin-polarized ELF_s (equation 4) and its usual functional form (equation 3) will be examined in terms of degree of the electron localization. Another purpose of the report is to explore how, from the total ELF, the electron localization can be evaluated in any subparts of the density.

II. ELF decomposition into density components

The total electron density can be trivially decomposed into orbitals components. Under the only constraints of the single or double occupation ε_i for each spatial molecular orbital φ_i (Hartree-Fock or Kohn-Sham formalisms), ρ can be written as a function of subshell electron densities of n_1 and n_2 occupied MOs:

$$\rho = \sum_{i=1}^{n} \varepsilon_i |\phi_i|^2 = \sum_{i=1}^{n_1} \varepsilon_i |\varphi_i|^2 + \sum_{i=n_1+1}^{n_2} \varepsilon_i |\varphi_i|^2 = \rho_1 + \rho_2 \quad (5)$$

With $n_1 + n_2 = n$.

Note that this decomposition does not restricted to only spin densities, any split of the total density chemically significant could be considered.
A dimensionless normalized quantity x can be expressed as follows:

$$x(\mathbf{r}) = \frac{\rho_1(\mathbf{r})}{\rho(\mathbf{r})} \text{ or } 1\text{-}x(\mathbf{r}) = \frac{\rho_2(\mathbf{r})}{\rho(\mathbf{r})} \quad (6)$$

x generally depends on the position **r** because the ratios ρ_1/ρ or ρ_2/ρ do not remain constant over the molecular space and consequently x changes from 1 ($\rho_1 = \rho$) to 0 ($\rho_2 = \rho$). Note that in this context, the kinetic energy density τ can also be trivially separated into two parts $\tau = \tau_1 + \tau_2$ such as:

$$\tau_1 = \frac{1}{2}\sum_{i=1}^{n_1} |\nabla\phi_i|^2 \text{ and } \tau_2 = \frac{1}{2}\sum_{i=n_1+1}^{n_2} |\nabla\varphi_i|^2$$

The von Weizsäcker kinetic energy density

Generally, τ^w of the total system differs from the summation of kinetic energies for each subsystem $\tau_1^w + \tau_2^w$. Hence, the decomposition of τ^w remains a tricky problem. The first step is to remark that τ^w can be split in the following way[28]:

$$\tau^w = \frac{1}{8}\frac{|\nabla(\rho_1+\rho_2)|^2}{\rho_1+\rho_2} = \frac{x}{8}\frac{|\nabla\rho_1|^2}{\rho_1} + \frac{(1\text{-}x)}{8}\frac{|\nabla\rho_2|^2}{\rho_2} + \frac{2\nabla\rho_1\nabla\rho_2}{8(\rho_1+\rho_2)} \quad (7)$$

Therefore, a term τ_c^w where ρ_1 and ρ_2 are mixed, can be underlined as the difference between the summation $\tau_1^w + \tau_2^w$ and the total τ^w:

$$\tau_c^w = \tau_1^w + \tau_2^w - \tau^w = \frac{1}{8}\frac{|\nabla\rho_1|^2}{\rho_1}(1\text{-}x) + \frac{1}{8}\frac{|\nabla\rho_2|^2}{\rho_2}x - \frac{2\nabla\rho_1\nabla\rho_2}{8\rho}$$

$$\tau_c^w = \frac{1}{8}\frac{(\rho_1+\rho_2)|(1\text{-}x)\nabla\rho_1 - x\nabla\rho_2|^2}{\rho_1\rho_2} \geq 0 \quad (8)$$

Interestingly, the equation (8) underlines that τ_c^w is a positive quantity which implies that $\tau^{Pauli} > (\tau_1^{Pauli} + \tau_2^{Pauli})$ underlying a small overestimation of the electron localization if the summation $\tau_1^w + \tau_2^w$ is used instead of the total τ^w. This result is illustrated in Figure 1 with $\rho_1=\rho_\alpha$ and $\rho_2=\rho_\beta$. Here, the mixed term appears as negligible in the core regions because ρ_α and ρ_β are equal (x becomes 0.5). In the valence regions, the loss of the mixed term becomes conspicuous (see Figure 1).

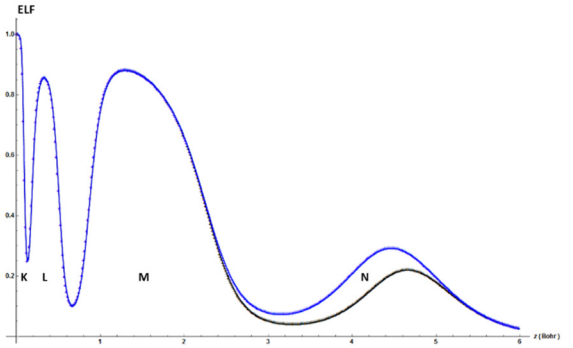


Figure 1: ELF values along the z axis of the K(^{2}S) atom calculated at the B3LYP /aug-cc-pVTZ level of theory. ELF (equation 3) is displayed in black while ELF without the mixed term τ_c^w is displayed in blue. The capital letters give the shells.

Generally, if x does not depend of **r,** namely that the ratio ρ_1/ρ_2 remains unchanged over the space, the equation (8) evidences that the mixed term is lost (τ_c^w =0) since $|\nabla\rho_1|$ = x $|\nabla\rho|$ and $|\nabla\rho_2|$ = (1- x) $|\nabla\rho|$, and thereby simplifying τ^w as the sum $\tau_1^W + \tau_2^W$. Note that applied to the spin-densities, this mixed term becomes zero for the closed-shell systems in which x=1/2 ($\rho_\alpha = \rho_\beta = \rho/2$) everywhere. It is worth noting that in practice, for most systems, τ_c^w remains generally very small with respect to kinetic energy densities because the subsystem densities are mainly distributed in different regions of the molecular space.

The HEG kinetic energy density

The decomposition of τ^h into density components is not a trivial problem because τ^h differs from the summation of kinetic energies for each subsystem. However, it has been previously shown that τ^h can be easily split as follows[28]:

$$\tau^h = c_f\,\rho^{5/3}$$

$$= c_f\,x^{5/3}\,\rho^{5/3} + c_f\,(1-x^{5/3})\,\rho^{5/3} = c_f\left(\rho_1^{5/3} + g(x)\,\rho_2^{5/3}\right) \quad (9)$$

where $g(x) = \frac{1 - x^{5/3}}{(1-x)^{5/3}}$. The plot of g(x) is displayed in Figure 2.

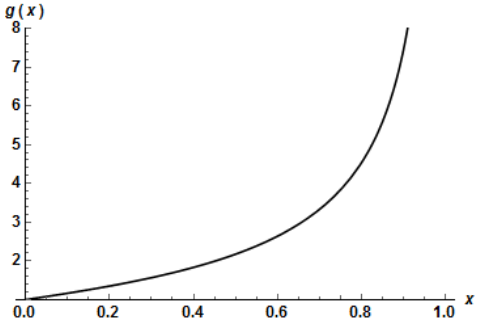


Figure 2: Plot of the g(x) function

As shown in Figure 2, *g*(0) is 1 and *g*(x) goes to infinity while *x* becomes 1. Actually, at the limit $x \to 1$, the quantity $g(x)\,\rho_2^{5/3}$ occuring in the equation (9) switch to 0 while *x* becomes 1 because ρ_2 becomes always zero faster than g(x) goes to infinity. In a similar manner to the von Weizsäcker quantity, a term τ_c^h where ρ_1 and ρ_2 are mixed, can be underlined as the difference between the summation $\tau_1^h + \tau_2^h$ and the total τ^h as follows:

$$\tau_c^h = \tau_1^h + \tau_2^h - \tau^h = 2^{2/3}c_f\,\rho_1^{5/3} + 2^{2/3}c_f\,\rho_2^{5/3} - \tau^h$$

$$= c_f\left(2^{2/3} - 1\right)\rho_1^{5/3} + c_f\left(2^{2/3} - g(x)\right)\rho_2^{5/3} \geq 0 \quad (10)$$

τ_c^h appears always positive even when x goes to 1 ($\rho_1 \approx \rho$, $g(x)\,\rho_2^{5/3} \to 0$). It becomes only zero when x=1/2. Thus, the equation (10) shows that $\tau^h < (\tau_1^h + \tau_2^h)$ underlying an overestimation of the electron localization if the summation $\tau_1^h + \tau_2^h$ is used instead of the total τ^h. Once again, this result is shown in Figure 3 where $\rho_1=\rho_\alpha$ and $\rho_2=\rho_\beta$. Note that the mixed term appears quite negligible in the core regions where x=1/2 since $\rho_\alpha = \rho_\beta$.

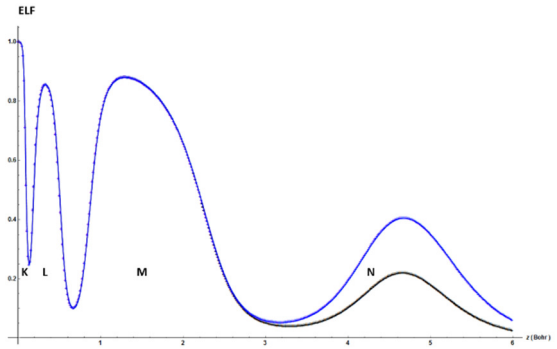


Figure 3: ELF values along the z axis of the K (^{2}S) atom calculated at the B3LYP /aug-cc-pVTZ level of theory. ELF (equation 3) is displayed in black while ELF without the mixed term τ_c^h is displayed in blue. The capital letters give the shells.

The polarized ELF

At this stage, one can easily grasp how density components play such a role in determining the degree of the electron localization measured by the total ELF (equation 3). Indeed, the kernel of ELF can be now related to its kinetic energy components:

$$\chi = \frac{\tau_1^{Pauli} + \tau_2^{Pauli} + \tau_c^{w}}{\tau_1^{h} + \tau_2^{h} - \tau_c^{h}} \geq \frac{\tau_1^{Pauli} + \tau_2^{Pauli}}{\tau_1^{h} + \tau_2^{h}} \quad (11)$$

The equation (11) is a decomposition of ELF into unmixed (τ_1^{Pauli}, τ_2^{Pauli} , τ_1^{h} , τ_2^{h}) and mixed (τ_c^{w} , τ_c^{h}) terms. It highlights that if both mixed terms are omitted, the degree of electron localization is overestimated. Applied to spin-densities ($\rho_1 = \rho_\alpha$, $\rho_2 = \rho_\beta$), the spin-polarized χ_s formula (equation 4) can be directly obtained from χ if these both mixed terms are dismissed. Nevertheless, the equation (11) shows that in the case of closed-shell (x =1/2, $\rho_\alpha = \rho_\beta = \rho/2$), the relation $\chi^s = \chi$ remains exactly verified since the mixed terms become exactly zero over the space. Beyond the connection between χ^s and χ, a polarized form of ELF taking account mixed terms, even approximatively, should be able to properly describe the degree of localization in the whole molecular space. Thus, a polarized ELF as close as possible to ELF_s, could be expressed as a sum of each Pauli kinetic energy weighted by x components where the HEG reference occuring in ELF_s remains unchanged:

$$\chi_p = \frac{2\left(x\,\tau_1^{Pauli} + (1\text{-}x)\,\tau_2^{Pauli}\right) + \varepsilon}{\tau_1^{h} + \tau_2^{h}} = \frac{2\left(x\,\tau_1^{Pauli} + (1\text{-}x)\,\tau_2^{Pauli}\right) + \varepsilon}{c_f\, 2^{2/3}\left(\rho_1^{5/3} + \rho_2^{5/3}\right)} \quad (12)$$

$ELF_p = (1+ \chi_p^{2})^{-1}$, ε being a shifting constant which constrains ELF_p to be less than 0.5 when $\rho \leq 10^{-3}$density. This constant was introduced for ELF (see the introduction section) in which $\varepsilon = 2.871.10^{-5}$. [25] In the case of ELF_p, $\varepsilon = 4.5574.10^{-5}[x^{5/3} + (1\text{-}x)^{5/3}]$. ELF and ELF_p go necessarily to zero for vanishing density (regions with numerical instabilities) whereas in its original definition (equations 1 and 3), ELF tends to 1 in low density regions. The factor 2 in the equation (12) holds the closed-shell connection since if x=1/2, χ_p is exactly equal to χ over the space. If x=0 or x=1, χ_p becomes proportional (factor 2) to the original expression of Becke and Edgecombe (equation 1).

Three examples of comparative behaviors of ELF_p, ELF_s and the ELF (equation 3) are displayed in Figure 4. We can notice that both ELF_p and ELF display very similar profiles, ELF_p appearing almost isotopological to ELF since the location and properties of critical points (local minima and maxima) are almost the same in the whole molecular space.

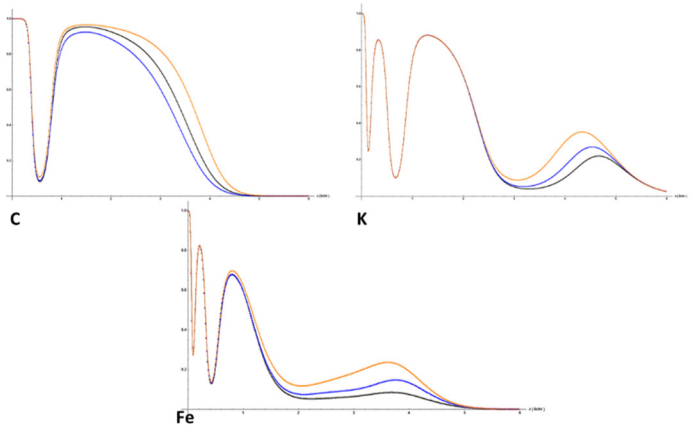


Figure 4: ELF values along the z axis of C (^{3}P), K (^{2}S) and Fe (^{5}D) atoms calculated at the B3LYP /aug-cc-pVTZ level of theory. ELF (equation 3), ELF_p (equation 12 with $\rho_1=\rho_\alpha$ and $\rho_2=\rho_\beta$) and ELF_s (equation 4) values are respectively displayed in black, blue and orange.

However, as regards the spin-polarized ELF_s (equation 4), the function can slightly differ from ELF in valence regions where the single electron character dominates. As discussed above, this is due to the overestimation of the degree of localization in ELF_s.

The distance between two minima of the considered function (ELF, ELF_p or ELF_s) can be defined as a shell radius and charts the frontier between the spherical basin centered on the maxima location. The shell population can be then computed by the integration of the density over the basin's volume. For closed-shell systems, radii and populations of three ELF, ELF_p and ELF_s are obviously the same (closed-shell connection). For open-shell systems, small differences are observed using the three formulas. The radius and the population of inner shells (K and L) have the same magnitude whatever the considered function. Conversely, the radius and the population of outer shells (M

and N) differ depending on the considered function. By way of example, consider the potassium atom K(^{2}S). The radius of the M shell decreases from 3.28 bohr for ELF to 3.06 bohr for ELF_s. A radius of 3.20 bohr is found for ELF_p which is close to that of ELF. Similar behavior is observed for the populations. The population of the M shell decreases from 8.05 *e* for ELF to 7.94 *e* for ELF_s. This population is 8.02 *e* for ELF_p which is close to that of ELF. Thus, these results show that ELF_p describes more adequately the degree of electron localization than ELF_s where mixed terms are dismissed.

III. Electron localization from density subsystems

As previously discussed by some authors[15,17], the total ELF (equations 3) lacks of assessment on the individual bonding pictures such as the conventional σ/π scheme. Of course, one could use separated ELF components (for example $ELF_{\alpha/\beta}$ or $ELF_{\sigma/\pi}$) to measure the localization in subparts of the total density. However, as seen from the above discussion, the ELF components cannot be, in general, properly connected to the total ELF without including mixed terms. In addition, the ELF component of a single orbital has no physical meaning (ELF becomes 1 in the whole space). In this case, ELF decays only due to the shifting constant introduced by Savin et al. Overall, a function χ_x quantifying a meaningful measure of electron localization for only a subpart of the total density system (for example ρ_1) needs to answer to following properties:

1. The localization is inversely proportional to the number of electrons delocalized in the subsystem, i.e. if $x\rightarrow 0$, the function χ_x goes to infinity and then $1/(1+\chi_x^2)$ goes to zero.

2. The closed-shell connection need to be sustained, i.e. $\chi_{x=}\chi$ when x=1/2.

These two criteria are fulfilled with the following equation:

$$\chi_x=\frac{\chi}{2\,x} \text{ and } ELF_x = \frac{1}{1+\chi_x{}^2} \qquad (13)$$

Indeed, ELF_x becomes zero when $x\rightarrow 0$. The factor 2 holds the closed-shell connection since if x=1/2, ELF_x = ELF. Note that ELF_x is also computed with the shifting constant introduced by Savin et al[25]. It is worth noting that if the subsystem involves only a single molecular orbital φ, i.e. $\rho_1=|\varphi|^2$, χ_x differs from zero while τ_1^{Pauli} becomes zero over the molecular space [8].

The calculations were performed on a set of prototype systems where the separation of group of molecular orbitals within their symmetry, is chemically intuitive. Figure 5 depicts the electron localization domains computed with ELF_x for selected orbital dissections: core/valence separation in the benzene ($\rho = \rho_c + \rho_v$), σ/π separation in the benzene ($\rho = \rho_\sigma + \rho_\pi$), separation of spin-densities in the radical C_6H_4 ($\rho = \rho_\alpha + \rho_\beta$).

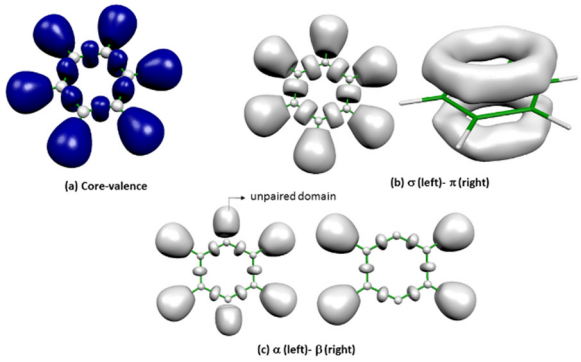


Figure 5. ELF_x localization domains (ELF=0.85 except for $ELF_{x,\pi}$ = 0.6). (a) Separation into core and valence regions of the benzene molecule. Light grey: $\rho_1=\rho_{core}$ and blue: $\rho_1=\rho_{valence}$. (b) Separation into σ and π regions of the benzene molecule. Left: : $\rho_1=\rho_\sigma$ and right : $\rho_1=\rho_\pi$ (c) Separation of density-spin components of the C_6H_4 molecule. Left: $\rho_1=\rho_\alpha$ and right: $\rho_1=\rho_\beta$.

One can see that in all cases, the ELF_x topologies match closely with the chemically meaningful pictures. By way of example, consider the α and β localization domains in the Phenyl radical molecule. We observe, in Figure 5, an agreement between the topological domains displayed by ELF_x and those of $ELF_{\alpha/\beta}$ components. They

clearly show the unpaired domains of α functions while these domains do not exist in β functions.

We now turn to the π localization domains in the benzene displayed in Figures 5 and 6.

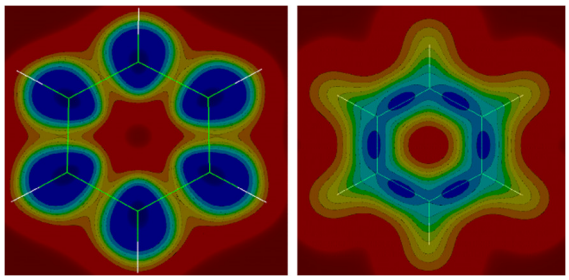


Figure 6. Compared localization domains of ELF_{π} (left) and $ELF_{x,\pi}$ (right) depicted in the molecular plane of the benzene molecule. Blue regions are domains of high electron localization while red regions are domains of low electron localization.

Regarding the topology of $ELF_{x,\pi}$, it corresponds to a typically delocalized double bond picture where the attractors (local maxima) of bonding basins C-C are located between the carbon atoms rather than on the carbon atoms. Note that this statement drawn from ELF_x differs from the topology of the single ELF_{π} component (see Figure 6) where the localization domains of C-C bonds are located on the carbon atoms above and below the molecular plane.

Further example of ELF_x can be gained in a context of frontier reactivity theory[26,29,30] with $\rho_1 = \varepsilon_{HOMO} |\varphi_{HOMO}|^2$ and $x = \varepsilon_{HOMO} |\varphi_{HOMO}|^2/\rho$. The ELF_x topology is then expected to simply stands for the contribution of the frontier orbital to the pair regions in the studied systems. Within a frozen orbital approximation, i.e. orbitals remaining unchanged upon addition and subtraction of one electron, ρ_1 is simply reduces to the Fukui function f^- which is a local descriptor of the nucleophilicity.[31-34] Overall, Fukui functions are powerful tools to get an insight into the reactivity since they allow to select the electrophilic and nucleophilic regions of the molecular space.

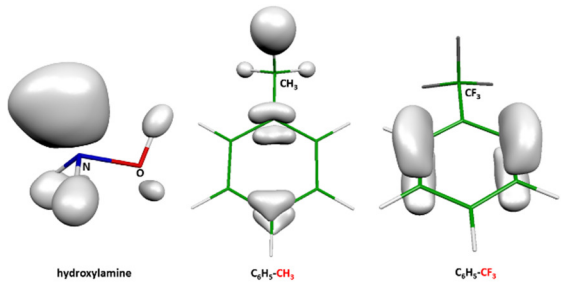


Figure 7. ELF_x localization domains built from the single Highest Occupied Molecular Orbital ($\rho_1 = 2 |\varphi_{HOMO}|^2$) for NH_2OH (ELF=0.6), Toluene (ELF=0.75) and Trifluorotoluene (ELF=0.75) molecules.

The electron localization domains of ELF_x for three selected systems are reported in Figure 7. For the NH_2OH molecule, the ELF_x topology yields non-bonding basins accounting for nitrogen and oxygen lone pairs, no N-O bonding oxygen basin was found. This can be conveniently interpreted by means of a bifurcation theory where the value of isosurfaces when basins begin to split (points of bifucation) are related to a measure of the electron localization and to the chemical interaction among the different basins.[25] Interestingly, the nitrogen and oxygen non-bonding basins presents a weak ELF_x bifurcation value of 0.66, thereby leaving a single nitrogen localization domain above the bifurcation value. In addition, the integration of the HOMO density $\int 2|\varphi_{HOMO}|^2 d\mathbf{r}$ was computed over the basin volumes (populations) for all the basins of NH_2OH. A population of 0.31 e was found for the oxygen non-bonding basin whereas a population of 1.26 e was found for the nitrogen non-bonding basin. A population close to 0.1 e was found for each hydrogen basin. Hence, it is clear from these findings, that nitrogen center is predicted to be more nucleophilic than those corresponding to the oxygen and the hydrogen centers. This outcome is consistent with the well-known reactivity of the hydroxylamine predicts by Fukui analyses [35,36]. This is also experimental evidenced that the nitrogen atom is the most reactive, at least, for the protonation process.[37]

The localization domains of ELF_x of $C_6H_5CH_3$ (*ortho-para* reactivity) and $C_6H_5CF_3$

(*meta* reactivity) are also displayed in Figure 7. Once again, excluding the ipso position of $C_6H_5CH_3$[20], the topology of ELF basins matches closely with the known local nucleophilicity of these compounds, notably predicts by the Fukui and the molecular orbital analyses[35]. Indeed, only localized valence basins are observed around carbons *ortho* and *para* for $C_6H_5CH_3$ while only basins are displayed around carbons *meta* for $C_6H_5CF_3$.

All Geometry optimizations were performed using the B3LYP hybrid functional[38] combined with the aug-cc-pVTZ basis set for all calculations. The DFT calculations have been performed using the GAUSSIAN09 program package.[39] Afterward, ELF calculations were carried out using a modified version of the TopMod and TopChem programs. ELF isosurfaces were drawn using the Molekel software.[40,41]

IV. Concluding Remarks

In summary, this work has introduced a decomposition of ELF obtained from an appealing scheme of kinetic energy components. The relationship between ELF and its usual spin-polarized formula, proposed by Kohout and Savin a few years ago, has been clarified by showing how the spin-polarized ELF can be obtained if mixed terms are omitted. Beyond spin-densities, a new ELF polarized formula was proposed. Regarding the degree of the electron localization measured in ELF, a localization function quantifying the measure of electron localization for only a subpart of the total system was introduced. The function could be useful to evaluate electronic properties which depend only on subparts of the density (aromatic character, radicals...) in various chemical systems and notably to be useful for exploring the local chemical reactivity of donor systems.

References

[1] B. Silvi, R. J. Gillespie, C. Gatti. In Comprehensive Inorganic Chemistry II (Second Edition); Poeppelmeier, K., Ed.; Elsevier: Amsterdam, 2013, p 187-226.

[2] B. Silvi, J. Pilme, F. Fuster, M. E. Alikhani. In Metal-Ligand Interactions; Russo, N., Salahub, D.,Witko, M., Eds.; Springer Netherlands, 2003, p 241-284.

[3] T. Zhang, W. Lei, P. Liu, J. A. Rodriguez, J. Yu, Y. Qi, G. Liu, M. Liu. J Phys Chem C 2016, 120(5), 2777-2786.

[4] L. A. Mancera, D. M. Benoit. J Phys Chem A 2015, 119(12), 3075-3088.

[5] M. Rahm. J Chem Theory Comput 2015, 11(8), 3617-3628.

[6] P. L. Ayers, R. J. Boyd, P. Bultinck, M. Caffarel, R. Carbó-Dorca, M. Causá, J. Cioslowski, J. Contreras-Garcia, D. L. Cooper, P. Coppens, C. Gatti, S. Grabowsky, P. Lazzeretti, P. Macchi, Á. Martín Pendás, P. L. A. Popelier, K. Ruedenberg, H. Rzepa, A. Savin, A. Sax, W. H. E. Schwarz, S. Shahbazian, B. Silvi, M. Solà, V. Tsirelson. Comput Theor Chem 2015, 1053, 2-16.

[7] A. Savin. Journal of Molecular Structure: THEOCHEM 2005, 727(1–3), 127-131.

[8] J. K. Burdett, T. A. McCormick. J Phys Chem A 1998, 102(31), 6366-6372.

[9] M. Kohout, R. F. Wagner, Y. Grin. Theor Chem Acc 2002, 108(3), 150-156.

[10] M. Kohout, A. Savin. J Comput Chem 1997, 18(12), 1431-1439.

[11] M. Amaouch, E. Renault, G. Montavon, N. Galland, J. Pilmé. In Applications of Topological Methods in Molecular Chemistry; Chauvin, R., Lepetit, C., Silvi, B.,Alikhani, E., Eds.; Springer International Publishing: Cham, 2016, p 553-582.

[12] J. Pilmé, E. Renault, T. Ayed, G. Montavon, N. Galland. J Chem Theory Comput 2012, 8(9), 2985-2990.

[13] A. D. Becke, K. E. Edgecombe. J Chem Phys 1990, 92(9), 5397-5403.

[14] P. Fuentealba, E. Chamorro, J. C. Santos. In Theoretical and Computational Chemistry; Alejandro, T.-L., Ed.; Elsevier, 2007, p 57-85.

[15] J. C. Santos, W. Tiznado, R. Contreras, P. Fuentealba. J Chem Phys 2004, 120(4), 1670-1673.

[16] J. Melin, P. Fuentealba. Int J Quantum Chem 2003, 92(4), 381-390.
[17] S. N. Steinmann, Y. Mo, C. Corminboeuf. Phys Chem Chem Phys 2011, 13(46), 20584-20592.
[18] J. C. Santos, J. Andres, A. Aizman, P. Fuentealba. J Chem Theory Comput 2005, 1(1), 83-86.
[19] M. Kohout. Int J Quantum Chem 2004, 97(1), 651-658.
[20] M. Kohout, F. R. Wagner, Y. Grin. Int J Quantum Chem 2006, 106(7), 1499-1507.
[21] F. R. Wagner, V. Bezugly, M. Kohout, Y. Grin. Chem Eur J 2007, 13(20), 5724-5741.
[22] A. Savin, O. Jepsen, J. Flad, O. K. Andersen, H. Preuss, H. G. von Schnering. Angew Chem Int 1992, 31(2), 187-188.
[23] C. Von Weizsacker. Zeitschrift für Physik 1935, 96(7), 431-458.
[24] E. Matito, B. Silvi, M. Duran, M. Solà. J Chem Phys 2006, 125(2), 024301.
[25] A. Savin, B. Silvi, F. Colonna. Can J Chem 1996, 74(6), 1088-1096.
[26] R. Parr, W. Yang. Density-Functional Theory of Atoms and Molecules; Oxford University Press: New York, 1994.
[27] M. Kohout, A. Savin. Int J Quantum Chem 1996, 60(4), 875-882.
[28] M. S. Miao. J Phys A: Math Gen 2001, 34(39), 8171.
[29] P. Geerlings, F. De Proft, W. Langenaeker. Chem Rev 2003, 103(5), 1793-1874.
[30] E. Chamorro, J. Melin. Journal of Molecular Modeling 2015, 21(3), 1-3.
[31] K. Fukui. In Orientation and Stereoselection; Springer Berlin Heidelberg: Berlin, Heidelberg, 1970, p 1-85.
[32] R. G. Parr, W. Yang. J Am Chem Soc 1984, 106(14), 4049-4050.
[33] W. Yang, R. G. Parr. Proceedings of the National Academy of Sciences 1985, 82(20), 6723-6726.
[34] P. Fuentealba, C. Cardenas, R. Pino-Rios, W. Tiznado. In Applications of Topological Methods in Molecular Chemistry; Chauvin, R., Lepetit, C., Silvi, B.,Alikhani, E., Eds.; Springer International Publishing: Cham, 2016, p 227-241.
[35] P. Fuentealba, E. Florez, W. Tiznado. J Chem Theory Comput 2010, 6(5), 1470-1478.
[36] E. Chamorro, M. Duque, C. Cárdenas, J. Santos, W. Tiznado, P. Fuentealba. J Chem Sci (Bangalore, India) 2005, 117(5), 419-424.
[37] F. Angelelli, M. Aschi, F. Cacace, F. Pepi, G. de Petris. J Phys Chem 1995, 99(17), 6551-6556.
[38] P. J. Stephens, F. J. Devlin, C. F. Chabalowski, M. J. Frisch. J Phys Chem 1994, 98(45), 11623-11627.
[39] M. J. Frisch, G. W. Trucks, H. B. Schlegel, G. E. Scuseria, M. A. Robb, J. R. Cheeseman, G. Scalmani, V. Barone, B. Mennucci, G. A. Petersson, H. Nakatsuji, M. Caricato, X. Li, H. P. Hratchian, A. F. Izmaylov, J. Bloino, G. Zheng, J. L. Sonnenberg, M. Hada, M. Ehara, K. Toyota, R. Fukuda, J. Hasegawa, M. Ishida, T. Nakajima, Y. Honda, O. Kitao, H. Nakai, T. Vreven, J. A. Montgomery Jr., J. E. Peralta, F. Ogliaro, M. J. Bearpark, J. Heyd, E. N. Brothers, K. N. Kudin, V. N. Staroverov, R. Kobayashi, J. Normand, K. Raghavachari, A. P. Rendell, J. C. Burant, S. S. Iyengar, J. Tomasi, M. Cossi, N. Rega, N. J. Millam, M. Klene, J. E. Knox, J. B. Cross, V. Bakken, C. Adamo, J. Jaramillo, R. Gomperts, R. E. Stratmann, O. Yazyev, A. J. Austin, R. Cammi, C. Pomelli, J. W. Ochterski, R. L. Martin, K. Morokuma, V. G. Zakrzewski, G. A. Voth, P. Salvador, J. J. Dannenberg, S. Dapprich, A. D. Daniels, Ö. Farkas, J. B. Foresman, J. V. Ortiz, J. Cioslowski, D. J. Fox. Gaussian, Inc.: Wallingford, CT, USA, 2009.
[40] P. Flukiger, H. P. Luthi, S. Portmann, J. Weber. Swiss Center for Scientific Computing: Manno, Switzerland, 2002.
[41] D. Kozlowski, J. Pilmé. J Comput Chem 2011, 32(15), 3207-3217.